JOURNAL OF SOLID STATE CHEMISTRY 50, 204–212 (1983)

Concentration Quenching of the Nd^{3+} Emission in Alkali Rare Earth Borates

J. MASCETTI, C. FOUASSIER, AND P. HAGENMULLER

Laboratoire de Chimie du Solide du CNRS, Université de Bordeaux I, 351, Cours de la Libération, 33405 Talence Cédex, France

Received April 27, 1983; in revised form July 18, 1983

Four new ternary compounds with compositions $Li_6Nd(BO_3)_3$, $Na_3Nd_2(BO_3)_3$, $Na_3Nd(BO_3)_2$, and $Na_{18}Nd(BO_3)_7$ have been found in the M_2O–Nd_2O_3–B_2O_3 systems, where M is either Li or Na. Concentration quenching of the neodymium emission in homologous lanthanum or gadolinium borates has been investigated. While in the $Li_6Gd(BO_3)_3$, $Na_3La_2(BO_3)_3$, and $Na_3La(BO_3)_2$ host lattices the quenching rate shows a quadratic dependence on Nd^{3+} concentration, as expected since the coordination polyhedra are connected by common faces or edges, in $Na_{18}La(BO_3)_7$ the luminescent lifetime is not influenced by neodymium concentration. Lifetimes and crystal field splitting of the J levels are compared to those of other oxide host lattices.

In most host lattices cross-relaxation processes cause strong concentration quenching of the Nd^{3+} emission (*1*). In 1972 Danielmeyer and Weber showed that in NdP_5O_{14} this phenomenon was considerably reduced (*2*). In the past decade a few other low concentration quenching materials have been discovered. Most of them are phosphates: $LiNdP_4O_{12}$, $KNdP_4O_{12}$ (*3*), $Na_2Nd_2Pb_6(PO_4)_6Cl_2$ (*4*); one is a borate: $NdAl_3B_4O_{12}$ (*5*). Owing to their high neodymium concentration, these crystals are characterized by a low pumping threshold of the stimulated emission (*6*).

The development of stoichiometric lasers has stimulated investigation into the nature of the quenching mechanisms and searches for new materials. Concentration quenching depends essentially on two parameters:

(i) the crystal field at the neodymium site: overlapping between emission and absorption lines which leads to cross-relaxation is reduced when crystal-field splitting of the J levels is small (*7, 8*);

(ii) the Nd^{3+}–Nd^{3+} distances: weak concentration quenching is only observed when the neodymium coordination polyhedra are isolated from each other. The absence of a common ligand and the large interatomic distances (>5 Å) reduce exchange coupling and multipolar interactions.

In all the abovementioned phases the isolated sites are situated in a three-dimensional covalent network. A large separation between Nd^{3+} ions can also be obtained in alkali-rich phases; such is the case for $K_5Nd(MoO_4)_4$ (*9*) and $Na_5Nd(WO_4)_4$ (*3*). In this paper we report the results of a study on the luminescent properties of Nd^{3+} in alkali rare earth borates. We have recently described the structure of the sodium neodymium borate $Na_3Nd(BO_3)_2$ (*10*). A lithium phase, $Li_3Nd_2(BO_3)_3$, was also known

0022-4596/83 $3.00

(*11*). An investigation of the M_2O (M = Li, Na)–Nd_2O_3–B_2O_3 systems showed the existence of three other borates with compositions $Li_6Nd(BO_3)_3$, $Na_3Nd_2(BO_3)_3$, and $Na_{18}Nd(BO_3)_7$. The concentration quenching of the neodymium emission has been investigated in solid solutions formed with homologous lanthanum or gadolinium phases.

I. Synthesis and Structural Features of Alkali Rare Earth Borates

The starting materials were the oxides M_2O (M = Li, Na), MBO_2, or B_2O_3 and Ln_2O_3 (Ln = La, Nd, Gd) (Rhône-Poulenc 99.99%). The mixture of oxides was put in an alumina crucible and heated in a nitrogen atmosphere.

I.1 The Sodium Rare Earth Borates

The Na_2O–Nd_2O_3–B_2O_3 system has been investigated in a temperature range extending from 500°C to the melting temperatures. $Na_3Nd_2(BO_3)_3$ and $Na_3Nd(BO_3)_2$ were obtained at 800°C, $Na_{18}Nd(BO_3)_7$ at 600°C. In the triangular diagram Na_2O–Nd_2O_3–B_2O_3 the three ternary phases lie on the line joining the Na_3BO_3 and $NdBO_3$ compositions. In view of the study of the concentration quenching, the existence of homologous lanthanum phases giving complete solid solutions was checked.

The $Na_3Ln_2(BO_3)_3$ (Ln = La, Nd) borates. $Na_3La_2(BO_3)_3$ and $Na_3Nd_2(BO_3)_3$ melt, respectively, at 1072 and 1042°C. Single crystals of $Na_3Nd_2(BO_3)_3$ were obtained from an equimolar mixture with $Na_4B_2O_5$, molten at 900°C, and slowly cooled down. Diffraction photographs showed an orthorhombic Laue symmetry *mmm* or *mm*2 and the systematic absences hkl: $k + l = 2n + 1$. The cell dimensions refined from powder data are given in Table I along with those of $Na_3La_2(BO_3)_3$. Also included in Table I are the data from the shortite $Na_2Ca_2(CO_3)_3$ (space group *Amm*2), whose diffraction pattern shows close similarities with that of the $Na_3Ln_2(BO_3)_3$ borates (*12*). It can be thought that the structure of the borate is closely related to that of the carbonate, the sodium in excess occupying a vacant site of the shortite structure. A preliminary structural investigation using powder data corroborates this assumption. Neodymium ions lie in the calcium sites. The NdO_7 polyhedra, linked by common faces, form chains along **c**.

TABLE I

CELL DIMENSIONS FOR THE $Na_3Ln_2(BO_3)_3$ (Ln = La,Nd) PHASES AND THE SHORTITE $Na_2Ca_2(CO_3)_3$

	$Na_3La_2(BO_3)_3$	$Na_3Nd_2(BO_3)_3$	$Na_2Ca_2(CO_3)_3$ (12)
a (Å)	5.120 ± 0.005	5.106 ± 0.005	4.99
b (Å)	11.276 ± 0.008	11.227 ± 0.008	10.99
c (Å)	7.184 ± 0.005	7.108 ± 0.005	7.11

Recall that it has been recently shown that shortite is a promising material for nonlinear optics (*13*).

The $Na_3Ln(BO_3)_2$ (Ln = La, Nd) borates. The structure of these borates has been described in a previous paper (*10*). The rare earth ions occupy one type of crystallographic sites with an eight-fold coordination. The minimum Nd–Nd distance, 4.15 Å, is observed in pairs of edge-sharing NdO_8 polyhedra.

The $Na_{18}Ln(BO_3)_7$ (Ln = La, Nd) borates. $Na_{18}Nd(BO_3)_7$ melts at 640°C. Crystals have been obtained from an equimolar mixture of $Na_{18}Nd(BO_3)_7$ and Na_3BO_3, heated at 725°C in a sealed gold tube and then cooled at 4°/hr. Preliminary X-ray investigations did not reveal any symmetry element. From the density, $d_{\text{meas.}} = 2.57$, an average Nd–Nd distance of 8.6 Å is inferred. We conclude that the neodymium coordination polyhedra are very likely isolated. Complete solid solution with the homologous lanthanum borate confirms that the two borates are isostructural. The interplanar spacings of the neodymium phase are listed in Table II.

TABLE II

X-RAY DIFFRACTION DATA FOR $Na_{18}Nd(BO_3)_7$

I/I_0	d (Å)	I	d (Å)
63	9.02	40	2.61
32	8.50	40	2.59
78	7.25	37	2.52
45	7.07	17	2.43
38	6.46	17	2.40
49	6.32	26	2.32
23	5.40	29	2.31
23	4.87	54	2.28
27	4.11	17	2.25
39	3.96	100	2.09
85	3.64	33	2.02
42	3.59	12	1.992
23	3.54	13	1.932
19	3.16	15	1.894
17	3.07	8	1.883
56	2.98	26	1.829
12	2.86	12	1.723
11	2.82	57	1.649
18	2.79	13	1.591
27	2.70	10	1.548

TABLE III

CELL DIMENSIONS FOR $Li_6Nd(BO_3)_3$

$a = 7.278 \pm 0.005$ Å
$b = 16.611 \pm 0.01$ Å
$c = 6.758 \pm 0.005$ Å
$\beta = 105.86 \pm 0.05°$

I.2 The Lithium Rare Earth Borates

The investigation of the Li_2O–Nd_2O_3–B_2O_3 system has been restricted to the Li_2O-rich part of the diagram. In addition to the previously known borate $Li_3Nd_2(BO_3)_3$, a new ternary phase of formulation $Li_6Nd(BO_3)_3$ was found. Attempts to prepare a phase of this type with lanthanum were unsuccessful. Up to melting the corresponding composition gives a mixture of Li_3BO_3 and $Li_3La_2(BO_3)_3$. A homologous phase was obtained with gadolinium. $Li_6Nd(BO_3)_3$ and $Li_6Gd(BO_3)_3$ are isostructural with the lithium holmium borate (*14*). The dimensions of the monoclinic unit cell (space group $P2_1/c$) obtained from the powder diffraction patterns are given in Table III for the neodymium phase. Edge-sharing LnO_8 polyhedra form isolated chains parallel to the c axis. The Nd–Nd intrachain distance is 3.95 Å.

More details about the structures of the alkali rare earth borates can be found in Ref. (*15*).

II. Optical Properties

Experimental

Absorption spectra were recorded with a Cary-17 spectrophotometer. Measurements of the fluorescence intensity were carried out on powder samples. Light from a xenon lamp was passed through a MTO A529 filter (bandpass region 500–600 nm). The emission was focused on the entrance slit of a Jobin-Yvon HRS 3 grating monochromator and detected by a Varian VPM-159A refrigerated InGaAsP photomultiplier tube.

The fluorescence lifetimes have been measured using the same system except that the source employed was a flashlamp or a 6-nsec pulsed nitrogen laser.

Concentration Quenching of the Neodymium Emission

As in $Li_3Nd_2(BO_3)_3$ the Nd^{3+} ions occupy two different crystallographic sites, the study was restricted to the four new borates. The ${}^4F_{3/2} \rightarrow {}^4I_{9/2}$ and ${}^4F_{3/2} \rightarrow {}^4I_{11/2}$ emissions at 78 K are shown in Fig. 1. The concentration dependence of the ${}^4F_{3/2} \rightarrow {}^4I_{11/2}$ emission intensity is given in Fig. 2. For the $Li_6Gd(BO_3)_3$, $Na_3La_2(BO_3)_3$, and $Na_3La(BO_3)_2$ host lattices, as generally observed, the intensity reaches a maximum at low Nd^{3+} concentration (about 5×10^{20} ions cm^{-3}) and then decreases rapidly. In con-

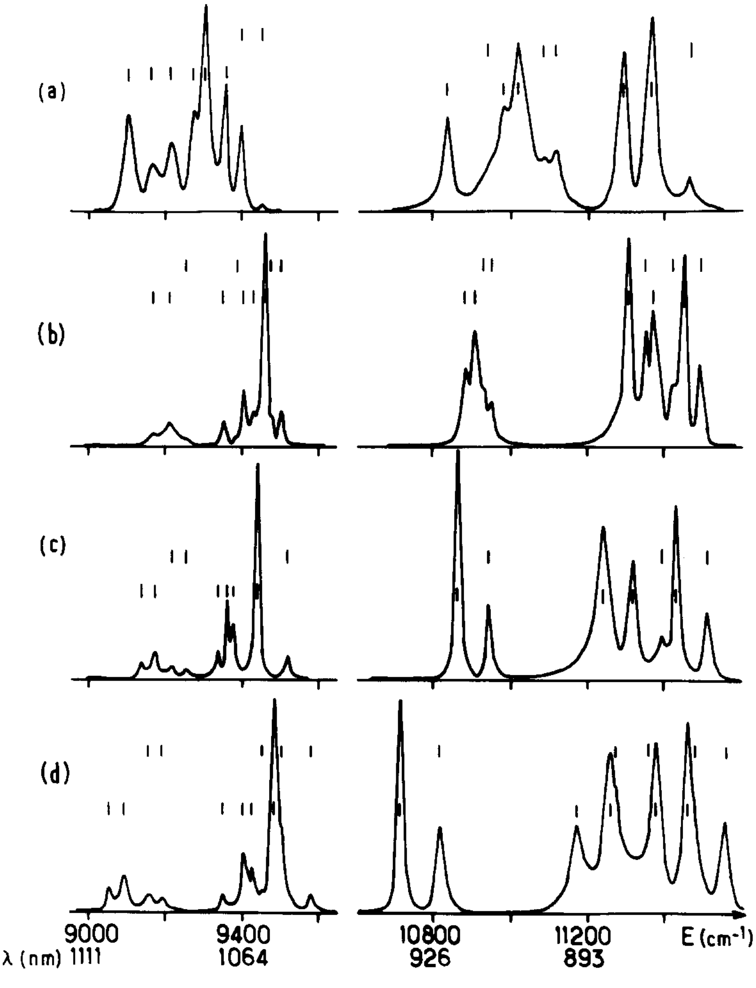

FIG. 1. Emission spectra of Nd^{3+} in Na$_3$(Nd$_{0.02}$La$_{0.98}$)$_2$(BO$_3$)$_3$ (a), Na$_3$Nd$_{0.05}$La$_{0.95}$(BO$_3$)$_2$ (b), Na$_{18}$Nd(BO$_3$)$_7$ (c), and Li$_6$Gd$_{0.925}$Nd$_{0.075}$(BO$_3$)$_3$ (d) at 77 K ($\lambda_{exc.}$ = 500 to 600 nm) (The dash associated with each emission line indicates the $^4F_{3/2}$ component from which the transition is issued.)

trast, for the Na$_{18}$La$_{1-x}$Nd$_x$(BO$_3$)$_7$ series, the intensity increases up to $x = 0.75$ and then remains practically constant up to $x = 1$. For this composition the neodymium concentration corresponds to 1.6×10^{21} ions cm^{-3}. The emission intensity is 75% of that of NdP$_5$O$_{14}$.

The decay of the luminescence has been investigated over a time range beginning 2 μsec after the pulse. No deviation from an exponential law has been detected. In Table IV the values of the lifetime in dilute medium (τ_0) and in the "stoichiometric" material are compared to those of various oxide host lattices. For all borates the observed τ_0 values are smaller than for other oxides.

As a consequence of the bonding covalency in phosphate groups, the mixing of the oxygen and Nd orbitals is weak, resulting in long lifetimes. The high value of τ_0 observed for the ordered perovskite Ba$_2$LaNbO$_6$ is due to small deviation from lo-

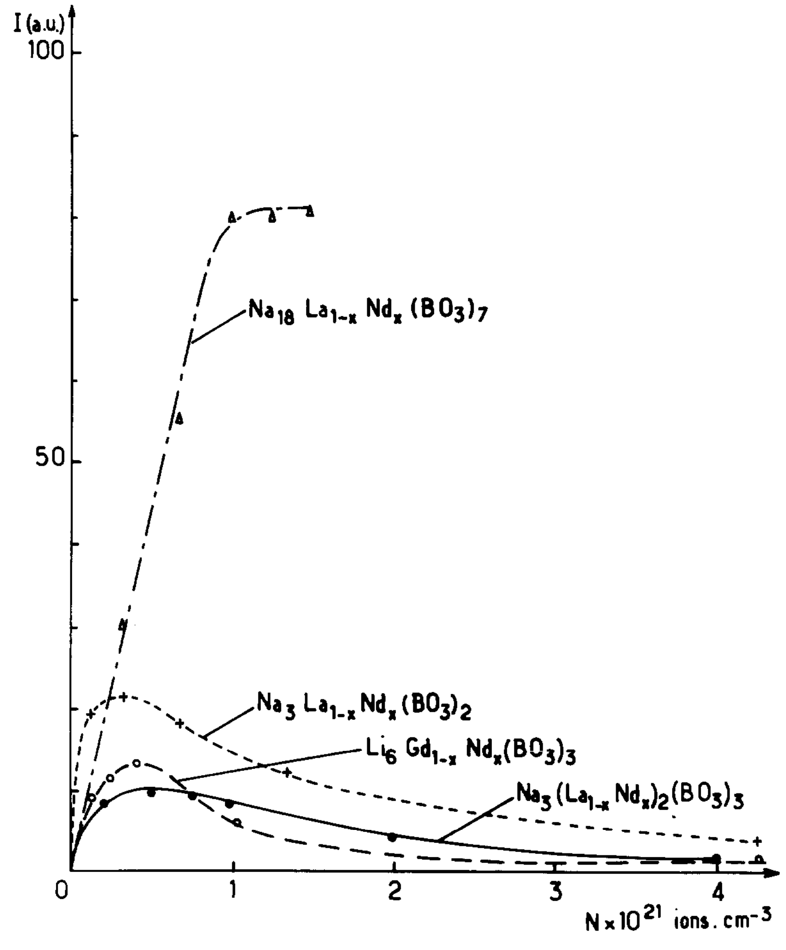

FIG. 2. Concentration dependence of the Nd^{3+} emission intensity in the borates $Li_6Gd_{1-x}Nd_x(BO_3)_3$, $Na_3(La_{1-x}Nd_x)_2(BO_3)_3$, $Na_3La_{1-x}Nd_x(BO_3)_2$, and $Na_{18}La_{1-x}Nd_x(BO_3)_7$.

cal inversion symmetry. The B–O bonds showing a high degree of covalency, the small values observed indicate that nonradiative processes contribute to the relaxation of the $^4F_{3/2}$ state. The BO_3^{3-} groups are characterized by high vibration frequencies, so multiphonon processes are probably the cause of the fast decays. The existence of nonradiative deexcitation processes at low concentration in the $Gd_{1-x}Nd_xAl_3B_4O_{12}$ borate has been demonstrated by Auzel: the radiative lifetimes obtained for a crystal of $NdAl_3B_4O_{12}$ from the oscillator strengths of the absorption lines amounts to 300 μsec compared to 50 μsec for the measured τ_0 value (*20*). Recent measurements in a borate glass give a quantum efficiency of only 22% (*29*).

Figure 3a shows that for the host lattices $Li_6Gd(BO_3)_3$, $Na_3La_2(BO_3)_3$, and $Na_3La(BO_3)_2$, the lifetime drops rapidly with increasing neodymium concentration. As shown for the $Na_3(La_{1-x}Nd_x)_2(BO_3)_3$ series in Fig. 3b, the quenching rate shows a quadratic dependence. Contrasting with this behavior, the lifetime of the $Na_{18}La_{1-x}Nd_x(BO_3)_7$ borate remains practically constant.

TABLE IV

COMPARISON OF THE Nd^{3+} FLUORESCENCE LIFETIME IN VARIOUS OXIDE HOST LATTICES

Oxide (Ref.)	Maximum Nd^{3+} concentration (at.cm^{-3}) (× 10^{21})	Number of nearest Nd^{3+} neighbors connected through common oxygen	Minimum Nd–Nd separation (Å)	Lifetime (μsec)		
				Low conc. (τ_0)	$x = 1$ (τ_f)	$\frac{\tau_0}{\tau_f}$
$Ba_2La_{1-x}Nd_xNbO_6$ (*18*)	3.2	0	6.07	572	14	41
$La_{1-x}Nd_xP_3O_9$(3)	5.8	2	4.23	375	5	75
$LiLa_{1-x}Nd_xP_4O_{12}$ (*3*)	4.4	0	5.94	325	135	2.4
$La_{1-x}Nd_xP_5O_{14}$ (*16*)	3.96	0	5.19	320	120	2.8
$KGd_{1-x}Nd_xP_4O_{12}$ (*3*)	4.1	0	6.66	275	100	2.7
$La_{1-x}Nd_xTa_7O_{19}$ (*19*)	3.1			275	125	2.2
$La_{1-x}Nd_xNa_5(WO_4)_4$ (*3, 26*)	2.6	0	6.45	220	85	2.6
$Na_2(La_{1-x}Nd_x)_2Pb_6(PO_4)_6Cl_2$ (*17*)	3.4			200	98	2.0
$NaLa_{1-x}Nd_xO_2$[a]	16.5	4	3.59	164	<5	>33
$Y_{1-x}Nd_xNbO_4$ (*17*)	10.5			113	4	28
$Na_3(La_{1-x}Nd_x)_2(BO_3)_3$[a]	9.8	3 + 2	3.66	82	<5	>16
$Na_3La_{1-x}Nd_x(BO_3)_2$[a]	6.7	3	4.15	88	<5	>18
$Na_{18}La_{1-x}Nd_x(BO_3)_7$[a]	1.6			80	80	1
$Li_6Gd_{1-x}Nd_x(BO_3)_3$[a]	5.1	2	3.94	82	5	16
$MgLa_{1-x}Nd_xB_5O_{10}$ (*28*)	6.4	2	3.99	55	<5	>11
$Gd_{1-x}Nd_xAl_3B_4O_{12}$ (*5*)	5.4	0	5.91	50	20	2.5

[a] This work.

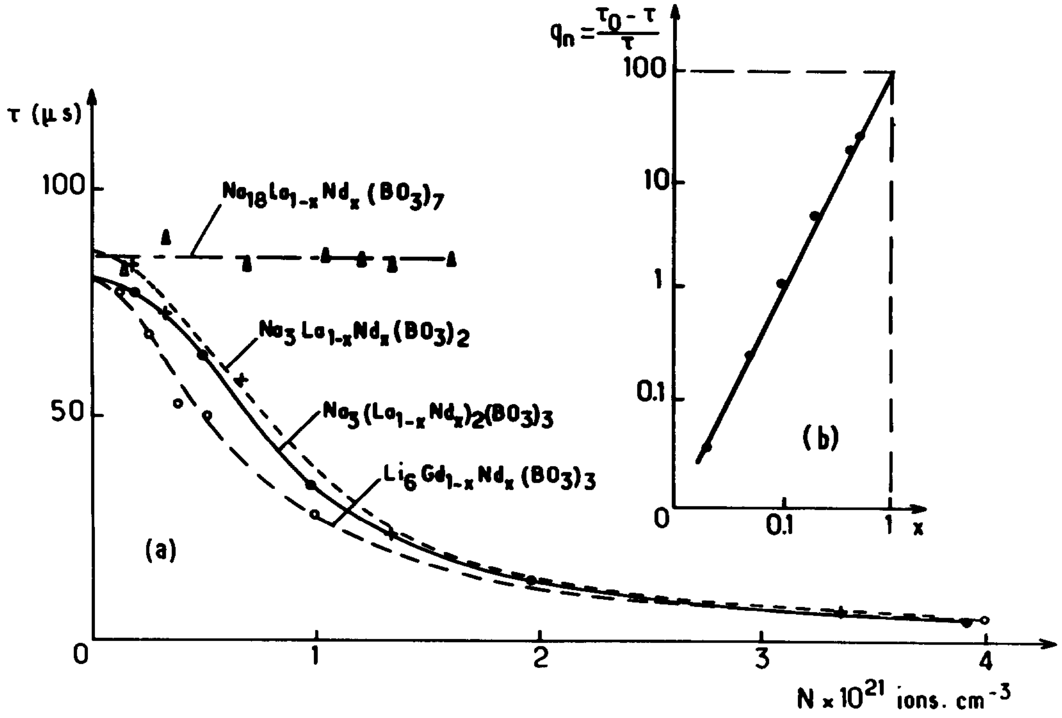

FIG. 3. (a) Concentration dependence of the lifetime of the $^4F_{3/2}$ emission in the alkali neodymium borates. (b) Variation of the normalized quenching constant $q_n = (\tau_0 - \tau)/\tau$ for $Na_3(La_{1-x}Nd_x)_2(BO_3)_3$ (τ_0 = lifetime at low concentration).

TABLE V

ENERGY OF THE STARK COMPONENTS OF THE LOWER Nd^{3+} LEVELS IN THE INVESTIGATED ALKALI NEODYMIUM BORATES (cm^{-1})

	$Li_6Gd_{1-x}Nd_x(BO_3)_3$ ($x = 0.075$)	$Na_3(La_{1-x}Nd_x)_2(BO_3)_3$ ($x = 0.02$)	$Na_3Nd(BO_3)_2$	$Na_{18}Nd(BO_3)_7$
$^4I_{9/2}$	0, 83, 199, 287, 746	0, 72, 350, 384, 530	0, 70, 145, 560, 562	0, 114, 188, 570
$^4I_{11/2}$	1977, 2035, 2060, 2109, 2368, 2407	2005, 2060, 2090, 2150, 2200, 2260	1966, 2012, 2042, 2092, 2240, 2284	1988, 2052, 2066, 2090, 2252, 2290
$^4I_{13/2}$			3920, 3940, 3980, 4038, 4175, 4275, 4304	
$^4I_{15/2}$			5803, 5855, 5918, 6024, 6375, 6442, 6471, 6512	
$^4F_{3/2}$	11,459, 11,559	11,364, 11,462	11,434, 11,480	11,428, 11,508

Note. The values have been derived from the emission spectra at 77 K, except for the $^4I_{13/2}$ and $^4I_{15/2}$ levels which are obtained from the absorption spectra of single crystals at 4 K.

Crystal Field Splitting of the J Levels

The energies of the lower levels determined from low temperature absorption or emission spectra are listed in Table V. In Table VI the splitting of the $^4I_{9/2}$, $^4I_{11/2}$, and $^4F_{3/2}$ levels is compared to that observed in other oxide host lattices. With the exception of $NdAl_3B_4O_{12}$, where the B–O bonds coexist with strong Al–O bonds, the borates generate a more intense crystal field than the phosphates do. The splitting of the ground state exceeds 470 cm^{-1}, which is the upper limit according to Auzel for low quenching (*8*). The complete determination of the lower energy levels for $Na_3Nd(BO_3)_2$ does show that cross-relaxation can result from the overlap of the $^4F_{3/2} \rightarrow {}^4I_{15/2}$ emission and the $^4I_{9/2} \rightarrow {}^4I_{15/2}$ absorption.

Discussion

As the probability of transfer of the excitation between two neodymium ions is higher than that of the cross-relaxation processes, concentration quenching is generally interpreted by a hopping model (*31, 32*). The law governing the concentration dependence of the nonradiative losses depends on the ratio of the probabilities W_{DA} and W_{DD} for donor–acceptor and donor–donor transfer, respectively:

$$W_{DA} = \frac{C_{DA}}{R^s} \qquad W_{DD} = \frac{C_{DD}}{R^s}$$

R is the distance between the interacting ions, $s = 6$ for dipole–dipole interactions. Here W_{DA} corresponds to the cross-relaxation probability. For a fraction of available sites occupied by neodymium ions lower than $x_c = \left(\frac{C_{DA}}{C_{DD}}\right)^{1/2}$, the initial part of the decay is governed by the direct donor–acceptor interactions (Förster decay) while the final part is determined by the migration of the excitation to the acceptor. The nonexponential initial part ends a short time after the excitation and has been rarely detected in oxides. The rate of nonradiative losses derived from the exponential final part is proportional to x^2. For $x > x_c$, the decay is exponential and the quenching rate varies linearly with neodymium concentration.

When the emission overlaps absorption lines, the probability for cross-relaxation is high, so a quadratic dependence is ob-

TABLE VI

CRYSTAL-FIELD SPLITTING OF THE $^4I_{9/2}$, $^4I_{11/2}$, AND $^4F_{3/2}$ LEVELS IN OXIDE HOST LATTICES

Host lattice	(Ref.)	Splitting of the *J* levels (cm^{-1})		
		$^4I_{9/2}$	$^4I_{11/2}$	$^4F_{3/2}$
NdP_5O_{14}	(*7*)	320	417	110
$Na_2Nd_2Pb_6(PO_4)_6Cl_2$	(*8*)	320		
$LiNdP_4O_{12}$	(*30*)	326	196	55
$KNdP_4O_{12}$	(*21*)	340	195	54
$NdAl_3B_4O_{12}$	(*22*)	285	173	67
$LaMgB_5O_{10}$	(*28*)	530	370	188
$Na_3La_2(BO_3)_3$	[a]	530	255	98
$Na_3La(BO_3)_2$	[a]	568	296	43
$Na_{18}La(BO_3)_7$	[a]	570	302	80
$Li_6Gd(BO_3)_3$	[a]	746	430	100
YVO_4	(*23*)	433	215	18
$NaLaO_2$	[a]	619		82
$LiYO_2$	(*24*)	639	467	194
Y_2O_3	(*25*)	841	466	
$Y_3Al_5O_{12}$	(*1*)	857	517	84
$LaTaO_4$				
Site I	(*27*)	940	592	210
Site II		830	603	100

[a] This work.

served up to high concentrations. Such is the case in the $Na_3La_2(BO_3)_3$, $Na_3La(BO_3)_2$, and $Li_6Gd(BO_3)_3$ host lattices.

For the three sodium borates, the splittings of the *J* levels are of the same order of magnitude. So the different behaviors should be ascribed to the variation of interatomic distances. In $Na_3Nd_2(BO_3)_3$, $Na_3Nd(BO_3)_2$, and $Li_6Nd(BO_3)_3$, the coordination polyhedra have common faces or edges and the interatomic distance is about 4 Å. In $Na_{18}Nd(BO_3)_7$, the average Nd–Nd distance is 8.6 Å, so that the coordination polyhedra are probably isolated. If the shortest Nd–Nd separation is close to this value, it markedly exceeds the values which characterize the other low-quenching oxides (Table IV). Interactions are therefore considerably reduced and the neodymium lifetime does not show significant variation with concentration.

Conclusion

The study shows that it is possible to get materials with high neodymium concentration (1.6×10^{21} at.cm^{-3}) without significant quenching when interatomic distances are of the order of 8 Å.

For host lattices showing a weaker probability of multiphonon processes than the borates investigated, the emission intensity would be comparable to that of the best low-quenching materials currently known. Compared to those, for laser emission such crystals would present several advantages: reduced thermal losses, lower probability of Auger recombination, and weaker self-absorption.

Acknowledgments

The authors are grateful to F. Guillen for technical support and J. P. Chaminade for crystal preparation.

References

1. H. G. DANIELMEYER, M. BLÄTTE, AND P. BALMER, *Appl. Phys.* **1,** 269 (1973).
2. H. G. DANIELMEYER AND H. P. WEBER, *IEEE J. Quantum Electron.* **8** (10), 805 (1972).
3. S. R. CHINN, H. Y.-P. HONG, AND J. W. PIERCE, *Laser Focus* **12** (5), 64 (1976).
4. J. P. BODIN, J. C. MICHEL, AND F. AUZEL, *J. Appl. Phys.* **50** (2), 641 (1979).
5. H. Y.-P. HONG AND K. DWIGHT, *Mater. Res. Bull.* **9,** 1661 (1974).
6. G. HUBER, *Curr. Top. Mater. Sci.* **4,** 1 (1980).
7. M. BLÄTTE, H. G. DANIELMEYER, AND R. ULRICH, *Appl. Phys.* **1,** 275 (1973).
8. F. AUZEL, *Mater. Res. Bull.* **14,** 223 (1979).
9. W. LENTH, H. D. HATTENDORF, G. HUBER, AND F. LUTZ, *Appl. Phys.* **17,** 367 (1978).
10. J. MASCETTI, M. VLASSE, AND C. FOUASSIER, *J. Solid State Chem.* **39,** 288 (1981).
11. G. K. ABDULLAEV AND K. S. MAMEDOV, *Sov. Phys. Crystallogr. Engl. Trans.* **22** (2), 154 (1977).
12. F. E. WICKMAN, *Ark. Mineral. Geol.* **1,** 95 (1949).
13. L. B. MEISNER, *Opt. Spektrosk.* **50** (2), 412 (1981).
14. G. K. ABDULLAEV, K. S. MAMEDOV, P. F. RZA-ZADE, S. A. GUSEINOVA, AND G. G. DZAFAROV, *Rus. J. Inorg. Chem.* **22** (12), 1765 (1977).
15. J. MASCETTI, Thèse d'Ingénieur-Docteur, Université de Bordeaux I, 1981.

16. B. C. Tofield, H. P. Weber, T. C. Damen, and G. A. Pasteur, *Mater. Res. Bull.* **9,** 435 (1974).
17. J. C. Michel, D. Morin, and F. Auzel, *C.R. Acad. Sci. (Paris)* **281,** 445 (1975).
18. P. Merchant, J. Grannec, J. P. Chaminade, and C. Fouassier, *Mater. Res. Bull.* **15,** 1113 (1980).
19. J. C. Michel, D. Morin, J. Primot, and F. Auzel, *C.R. Acad. Sci. (Paris)* **284,** 555 (1977).
20. F. Auzel, private communication.
21. C. Gueugnon and J. P. Budin, *IEEE J. Quantum Electron.* **16,** 94 (1980).
22. G. Winzer, P. G. Möckel, and W. W. Krühler, *IEEE J. Quantum Electron.* **14,** 840 (1978).
23. N. Karayianis, C. A. Morrison, and D. E. Wortman, *J. Chem. Phys.* **62,** 4125 (1975).
24. V. A. Antonov, P. A. Arsenev, S. A. Vakhidov, E. M. Ibragimona, and D. S. Petrova, *Phys. Status Solidi A* **41,** 45 (1977).
25. J. Stone and C. A. Burrus, *J. Appl. Phys.* **49,** 2281 (1978).
26. H. Y.-P. Hong and K. Dwight, *Mater. Res. Bull.* **9,** 775 (1974).
27. M. G. Zuev, F. A. Rozhdestvenskii, and E. I. Krylov, *Sov. Phys. Solid State Engl. Trans.* **16,** 613 (1974).
28. B. Saubat, Thèse, Université de Bordeaux I, 1980.
29. Gan Fuxi, Chen Shu Chun, and Hu Hefang, *Sci. Sin.* **24,** 1096 (1981).
30. K. Otsuka, T. Yamada, M. Saruwatari, and T. Kimura, *IEEE J. Quantum Electron.* **11,** 330 (1975).
31. Y. K. Voron'ko, T. G. Mamedov, V. V. Osiko, A. M. Prokhorov, V. P. Sakun, and I. A. Shcherbakov, *Sov. Phys. JETP Engl. Trans.* **44,** 251 (1976).
32. B. I. Denker, V. V. Osiko, A. M. Prokhorov, and I. A. Shcherbakov, *Sov. J. Quantum Electron.* **8,** 485 (1978).